

# Temporal Sparse Adversarial Attack on Sequence-based Gait Recognition

Ziwen He<sup>1,2</sup>, Wei Wang<sup>2</sup>, Jing Dong<sup>2</sup> & Tieniu Tan<sup>2</sup>

<sup>1</sup> School of Artificial Intelligence, University of Chinese Academy of Sciences

<sup>2</sup> Center for Research on Intelligent Perception and Computing, NLPR, CASIA  
ziwen.he@cripac.ia.ac.cn, {wwang,jdong,tnt}@nlpr.ia.ac.cn

## Abstract

*Gait recognition is widely used in social security applications due to its advantages in long-distance human identification. Recently, sequence-based methods have achieved high accuracy by learning abundant temporal and spatial information. However, their robustness under adversarial attacks has not been clearly explored. In this paper, we demonstrate that the state-of-the-art gait recognition model is vulnerable to such attacks. To this end, we propose a novel temporal sparse adversarial attack method. Different from previous additive noise models which add perturbations on original samples, we employ a generative adversarial network based architecture to semantically generate adversarial high-quality gait silhouettes or video frames. Moreover, by sparsely substituting or inserting a few adversarial gait silhouettes, the proposed method ensures its imperceptibility and achieves a high attack success rate. The experimental results show that if only one-fortieth of the frames are attacked, the accuracy of the target model drops dramatically.*

## 1. Introduction

Gait recognition is designed to automatically identify people according to their way of walking. Compared to traditional biometric information such as fingerprints or irises, gaits can be obtained at long distances without the cooperation of subjects. As a result, gait recognition is widely applied in remote visual surveillance solutions. In recent years, numerous gait recognition methods [32, 29, 13, 31, 18] have been proposed; they have achieved a high recognition accuracy. However, the security of gait recognition algorithms against malicious attacks has not been thoroughly studied. Limited work [15, 6, 11, 10] has studied the robustness of gait recognition to spoofing attacks, which aim to gain illegitimate access to the target gait recognition models.

In this paper, we investigate the security of gait recognition models subjected to adversarial attacks [28, 8]. Differ-

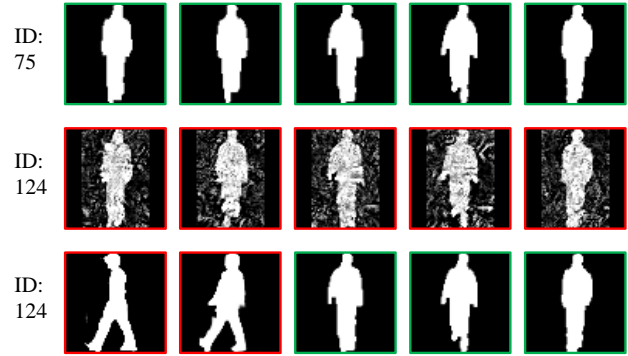


Figure 1. **Top row**: the original examples. **Middle row**: the perturbation-based adversarial examples. **Bottom row**: the temporal sparse adversarial examples. Adversarial examples are generated by running a targeted adversarial attack (the source ID is 75 and the target ID is 124) with different methods. The red bounding box represents the modified example, while the green bounding box represents the original example. The middle row directly transfers adversarial attack methods in image classification to gait recognition, causing all of the frames to be perturbed and imperceptibility decreased. The bottom row only has the first two frames modified. Besides, the modified frames maintain a gait appearance, so it is not easy for humans to distinguish whether they are adversarial examples or not.

ent from typical spoofing attacks, adversarial attacks aim to imperceptibly (i.e., without incurring visual cues) disable the gait recognition model (nontargeted attack) or gain illegitimate access by misleading the system to recognise as a target ID (targeted attack). Recently, adversarial attacks have been investigated including attacks on image classification [28, 8], object detection [33], face recognition [25], etc. However, for gait recognition, to the best of our knowledge, a meaningful attempt has not been reported, yet. A very likely reason is that the popular adversarial attack methods on image classification, like Fast Gradient Sign Method (FGSM) [8] and Projected Gradient Descent (PGD) [19], are not suitable to directly applied to gait recognition. Firstly, for sequence-based methods that

take a sequence of silhouettes segmented from the original video as input, perturbations added on the source video do not work. This is due to the signal processing these approaches require. Secondly, even if attackers have access to modify the probes, adding a norm-constrained perturbation to the original gait silhouette destroys the imperceptibility. This is illustrated in the second row of Fig. 1.

More specifically, this work focuses on the sequence-based methods [31, 18, 3]. Compared to template-based methods [32, 29, 13], in which temporal information is difficult to preserve, sequence-based methods are better at extracting dynamic clues from silhouette frames with deep neural networks (DNNs). As a result, these methods have a higher gait recognition accuracy. However, the DNN-extracted temporal features may be vulnerable to adversarial attacks. To verify this hypothesis, we propose a novel temporal sparse adversarial attack method for the gait recognition system.

We have two primary intuitions that are illustrated in Fig. 1. Firstly, the input of gait recognition models is a sequence of silhouette frames, rather than a single image for the image classification models. Therefore, to better achieve its imperceptibility, only a few frames may be modified in our attack. This ensures sparsity on the temporal domain. Secondly, motivated by unrestricted adversarial examples [2], crafting an unrestricted adversarial gait silhouette via deformation better achieves imperceptibility than adding norm-bounded perturbations. Moreover, adversarial silhouettes generated by the proposed method can easily be extended to valid video frames. This enables a practical threat to gait recognition systems.

The main contributions of this paper are as follows:

- To the best of our knowledge, we are the first attempt to address adversarial attacks on sequence-based gait recognition. We propose a novel temporal sparse adversarial attack specifically designed to target gait recognition methods. The proposed method simultaneously achieves a high attack success rate and satisfactory imperceptibility.
- Extensive experiments show the vulnerability of existing sequence-based gait recognition systems. We also investigate the difference between sequence-based and template-based gait recognition methods under our proposed attack method. The results indicate that sequence-based deep learning methods have little adversarial robustness despite their high accuracy.

## 2. Related work

### 2.1. Gait recognition

Gait recognition can generally be grouped into two categories, template-based [32, 29, 13] and sequence-based [31,

18]. The former category is composed of two main steps: template generation and matching. In the first step, human silhouettes are compressed into one template. For example, GEINet [26] and GaitGAN [34] use the gait energy image (GEI) [12] as the template. In the second step, the similarity between pairs of templates is evaluated, e.g., by the Euclidean distance. The latter category directly captures dynamic clues from the sequence of silhouette frames. This category includes 3D CNN-based approaches [31], LSTM-based approaches [18], and GaitSet [3]. Currently, GaitSet achieves the state-of-the-art gait recognition results on the CASIA-B [35] dataset.

### 2.2. Adversarial attack

Let  $x \in \mathbb{R}^m$  denote an input to a classifier  $f : \mathbb{R}^m \rightarrow \{1, 2, \dots, k\}$ , and assume the attacker has full knowledge of  $f$ . The goal of a nontargeted adversarial attack is to find the corresponding adversarial example  $x^* \in \mathbb{R}^m$  satisfying  $f(x^*) \neq f(x)$  with the constraint  $\|x^* - x\| \leq \epsilon$ , where  $\epsilon$  is a small constant. For targeted attack, the  $x^* \in \mathbb{R}^m$  aims to satisfy  $f(x^*) = t$ , where  $t$  is the target label. In this additive perturbation approach, different norms  $\|\cdot\|$  have been used, such as  $l_1$  [17],  $l_2$  [21] or  $l_0$  [22]. A series of methods have been proposed such as FGSM [8], PGD [19], and MIFGSM [5]. The adversarial perturbations are typically restricted to a small norm.

In contrast, unrestricted adversarial examples [2, 27, 24] are constructed entirely from scratch instead of perturbing existing data points by a small amount. Poursaeed et al. [24] manipulate stylistic and stochastic latent variables that are fed into the StyleGAN [16] to generate an unrestricted adversarial image to mislead a classification model. Similarly, we adopt a generative model to generate an adversarial high-quality gait silhouette. Here, we extend the approach to include the temporal domain. Instead of perturbing each frame, we sparsely generate adversarial frames to alert or insert into the original gait sequence.

In addition, additional approaches are available in the literature on adversarial attacks via action recognition [30, 4]. Wei et al. [30] utilize  $l_1$  norm across frames to ensure the sparsity of adversarial perturbations on videos. A similar mask-based method is applied in our attack to control the sparsity. Chen et al. [4] propose a new adversarial attack that appends a few dummy frames to a video clip and then adds adversarial perturbations only on these new frames. In our attack, we also explore the strategy of inserting frames into gait sequences. Both methods [30, 4] achieve a superior success rate on attacking temporal sequences. Nonetheless, their methods focus on the norm-bounded perturbations and cannot be directly transferred to the gait recognition task for the reason presented in Sec. 1.

### 2.3. Generative adversarial network

Image generation is highly related to our task. A core challenge is generating silhouettes or video frames that are visually realistic. Generative adversarial network (GAN) [7] achieves impressive results in image synthesis and thus is applied in our method. Wasserstein GAN (WGAN) [1] is an important extension of GAN which improves image quality and stabilizes training. WGAN-GP [9] uses a gradient penalty to further improve the loss function. We use the WGAN-GP in the silhouette generation.

Another related study is the pixel-to-pixel generation approach [14], which is based on a type of conditional GANs for which both input and output are images. SPADE [23] is a method based on conditional normalization, and it can convert the segmentation map into a photo-realistic image. This is suitable for our silhouette to video frame generation. In this paper, although the adversarial frames are hard to detect due to the temporal sparsity, we still generate visually convincing frames for better imperceptibility in the spatial domain. Successfully fooling recognition systems in such a case demonstrates the effectiveness of our method.

## 3. Methodology

### 3.1. Problem formulation

Let  $\mathbf{X} \in \mathbb{R}^{N \times W \times H \times C}$  denote a clean silhouette sequence, and  $\mathbf{X}^* \in \mathbb{R}^{N \times W \times H \times C}$  denote its adversarial sequence, where  $N$  is the number of frames, and  $W, H, C$  are the width, height, and channel for a specific frame, respectively.

The nontargeted adversarial sequence  $\mathbf{X}^*$  is the solution of the following objective function:

$$\arg \min_{\mathbf{X}^*} \lambda \mathcal{C}(\mathbf{X}, \mathbf{X}^*) - \mathcal{L}_{\cos}(f(\mathbf{X}), f(\mathbf{X}^*)) \quad (1)$$

where  $\lambda$  is a weight that balances the two terms in the objective function and  $f$  is a gait recognition model that outputs the computed features of silhouette sequences. In addition,  $\mathcal{L}_{\cos}$  is the loss function to measure the cosine similarity between the ground truth sequence and the adversarial sequence;  $\mathcal{C}(\mathbf{X}, \mathbf{X}^*)$  is a distortion measurement to evaluate the difference between the original sequence and its adversarial sequence. For a perturbation-based attack, it is often defined as the  $l_p$  norm  $\|\mathbf{X}^* - \mathbf{X}\|_p$ . For our attack, we define a new measurement as

$$\mathcal{C}(\mathbf{X}, \mathbf{X}^*) = \sum_{n \in \Phi} (o(X_n) - o(X_n^*))^2 \quad (2)$$

where  $o$  is the oracle to decide whether the image is a reasonable gait silhouette and similar to its counterpart. As unrestricted adversarial examples [2], the adversarial frames in our attack are expected to maintain a gait appearance even

though they may have a large perturbation at the pixel-level.  $\Phi$  is a subset within the set of frame indices.

For clarity, we describe our method based on nontargeted setting. Our method can be easily generalized to targeted setting. The objective for finding an adversarial sequence misclassified as a target ID  $t$  is to minimize the loss function

$$\arg \min_{\mathbf{X}^*} \lambda \mathcal{C}(\mathbf{X}, \mathbf{X}^*) + \mathcal{L}_{\cos}(f(\mathbf{X}_t), f(\mathbf{X}^*)) \quad (3)$$

where  $\mathbf{X}_t$  is a sequence of ID  $t$ .

### 3.2. Temporal sparse attack

In our new measurement (2), the supervision of the oracle is of vital importance to improve the imperceptibility in the spatial domain. However, the objective function Eq.(1) is difficult to optimize. Thus, we use a well-trained generator to craft adversarial frames as in Poursaeed et al. [24]. The pipeline of our attack is shown in Fig. 2.

To control the temporal sparsity, similar to [30], we denote the temporal mask as  $\mathbf{M} \in \{0, 1\}^{N \times W \times H \times C}$ . We let  $\Omega = \{1, 2, \dots, N\}$  be the set of frame indices,  $\Phi$  be a subset within  $\Omega$  having  $K$  elements randomly sampled from  $\Omega$ , and  $\Psi = \Omega - \Phi$ . The selection of  $\Phi$  introduces randomization to make the crafted adversarial sequence more difficult to detect. If  $n \in \Phi$ , we set  $M_n = 0$ , and if  $n \in \Psi$ ,  $M_n = 1$ , where  $M_n \in \{0, 1\}^{W \times H \times C}$  is the  $n$ -th frame in  $\mathbf{M}$ . The sparsity is computed as  $S = K/N$ .

Denote the latent variables input into the generator as  $\mathbf{Z} \in \mathbb{R}^{N \times V}$ , where  $V$  is the dimension of each latent variable.  $G$  is a pre-trained generator on a gait silhouette dataset. Let  $\mathcal{M}$  be the natural gait silhouette manifold in  $\mathbb{R}^{W \times H}$ . In most generative models, a simple random sample  $\mathbf{Z}$  drawn from the standard Gaussian distribution does not guarantee that  $G(\mathbf{Z}) \in \mathcal{M}$ . To ensure the high quality of generated silhouettes, we must be in a region of the latent space with high probability. Inspired by Menon et al. [20], we replace the Gaussian prior on  $\mathbb{R}^V$  with a uniform prior on  $\sqrt{V}\mathbb{S}^{V-1}$ , where  $\mathbb{S}^{V-1} \subset \mathbb{R}^V$  is the unit sphere in the  $V$  dimensional Euclidean space. The adversarial sequence is obtained by

$$\mathbf{X}^* = \mathbf{M} \cdot G(\mathbf{Z}) + (\mathbf{1} - \mathbf{M}) \cdot \mathbf{X} \quad (4)$$

We name this method as a **frame-alteration attack**. Instead of modifying frames, a **frame-insertion attack** inserts frames into the original sequence to obtain the adversarial sequence  $\mathbf{X}^* \in \mathbb{R}^{(N+\Delta N) \times W \times H \times C}$ .

For the well trained generator  $G$ , all of the generated images  $G(\mathbf{Z})$  must be classified by the oracle as gait silhouettes, i.e.,  $\mathcal{C}(\mathbf{X}, \mathbf{X}^*) = 0$ . To ensure this, we use a trained discriminator  $D$  to supervise the generated silhouettes. The discriminator outputs the value one when the inputs are from the natural manifold; otherwise, the value zero is output. We make sure  $G(\mathbf{Z})$  keeps a high probability of

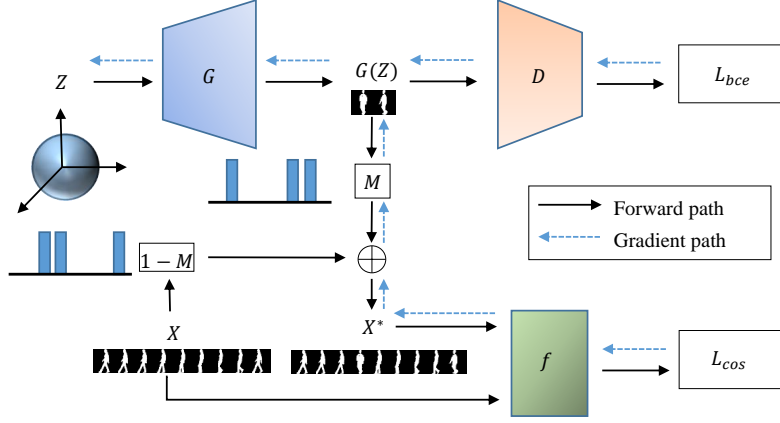


Figure 2. The pipeline of our attack approach. The trained generator  $G$  is used to generate high-quality gait silhouette image for imperceptibility on frame level. The mask  $M$  is used to achieve temporal sparsity for imperceptibility on the sequence level.

sampling from the natural manifold by utilizing the binary cross entropy (BCE) loss. Thus, our objective function in Eq.(1) is equal to optimizing  $Z$  to maximize the following loss

$$\mathcal{L} = \mathcal{L}_{cos}(f(\mathbf{X}), f(\mathbf{X}^*)) + \lambda \mathcal{L}_{bce}(D(G(\mathbf{Z})), 1) \quad (5)$$

$\lambda$  is a hyper-parameter to establish a trade-off between two terms. By performing a gradient ascent in the latent variable space of the generator, the corresponding  $Z$  that maximizes the final loss in Eq.(5) can be found. Without loss of generality, we adopt the MIFGSM [5] to attack  $f$  as follows.

$$\mathbf{g}_{(t+1)} = \mu \cdot \mathbf{g}_{(t)} + \frac{\nabla_{\mathbf{Z}_{(t)}} \mathcal{L}}{\|\nabla_{\mathbf{Z}_{(t)}} \mathcal{L}\|_1} \quad (6)$$

$$\mathbf{Z}_{(t+1)} = \mathbf{Z}_{(t)} + \epsilon \cdot \text{sign}(\mathbf{g}_{(t+1)}) \quad (7)$$

where  $\mu$  is the decay factor,  $\epsilon$  is the step size, and  $t$  represents the  $t$ -th iteration. Algorithm 1 shows the proposed temporal sparse adversarial attack.

### 3.3. Video generation

The above generation process only considers silhouette images. To show our method can successfully threaten other practical applications, we extend it to the generation of a valid video. This can be regarded as a pixel-to-pixel image generation task. Specifically, we apply the popular SPADE [23] in our experiments. The whole pipeline is shown in Fig.3.

Denote the source silhouette as  $L_s \in \mathbb{R}^{W \times H}$  and the source video frame as  $I_s \in \mathbb{R}^{W \times H}$ . We train a pix-to-pix generator  $G_p$  with paired data  $(I_s \times L_s, L_s)$ . In the attack

---

#### Algorithm 1 Temporal Sparse Adversarial Attack

---

**Input:** A gait recognition model  $f$ ; a generator  $G$ ; a discriminator  $D$ ; a silhouette sequence  $\mathbf{X}$ ; iterations  $T$  and decay factor  $\mu$ ; sparsity  $S$ ; step size  $\epsilon$ ; latent space dimension  $V$ ; a hyper-parameter  $\lambda$ .

**Output:** An adversarial silhouette sequence  $\mathbf{X}^*$ .

- 1:  $\mathbf{g}_0 = 0$ ;  $\mathbf{X}_0^* = \mathbf{X}$ ;  $\mathbf{Z}_0 \sim \sqrt{V} \mathbb{S}^{V-1}$ , where  $\mathbb{S}^{V-1}$  is the unit sphere space.
  - 2: Compute the mask  $M$  according to the sparsity  $S$ , details are in the text;
  - 3: **for**  $t = 0$  to  $T - 1$  **do**
  - 4:   Input  $\mathbf{Z}_t$  into the generator  $G$  and obtain the images  $G(\mathbf{Z}_t)$ ;
  - 5:   Compute the adversarial sequence as  $\mathbf{X}_t^* = M \cdot G(\mathbf{Z}_t) + (1 - M) \cdot \mathbf{X}$ ;
  - 6:   Compute the loss  $\mathcal{L}$  in Eq.(5);
  - 7:   Update  $\mathbf{g}_{(t+1)}$  by accumulating the velocity vector in the gradient direction as Eq.(6);
  - 8:   Update  $\mathbf{Z}_{(t+1)}$  by applying the clipped gradient as Eq.(7);
  - 9: **end for**
  - 10: **return**  $\mathbf{X}^* = M \cdot G(\mathbf{Z}_T) + (1 - M) \cdot \mathbf{X}$ .
- 

process, we feed the adversarial silhouette  $L_a$  into the generator. The generated image  $G_p(L_a)$  is supposed to contain a subject; there is no background scene. We paste the generated image on the background image  $I_b$  with the formulation  $I_a = I_b \times L_s + G_p(L_a)$ . Then, we insert the obtained adversarial frame into the source video or substitute a frame with it to generate the fake video. Though this method does not ensure spatial-temporal continuity between the adjacent real frames and adversarial frames, the modified frames are imperceptible due to the temporal sparsity. On the other hand, the modified frame keeps the same background, which is enough to deceive segmentation al-

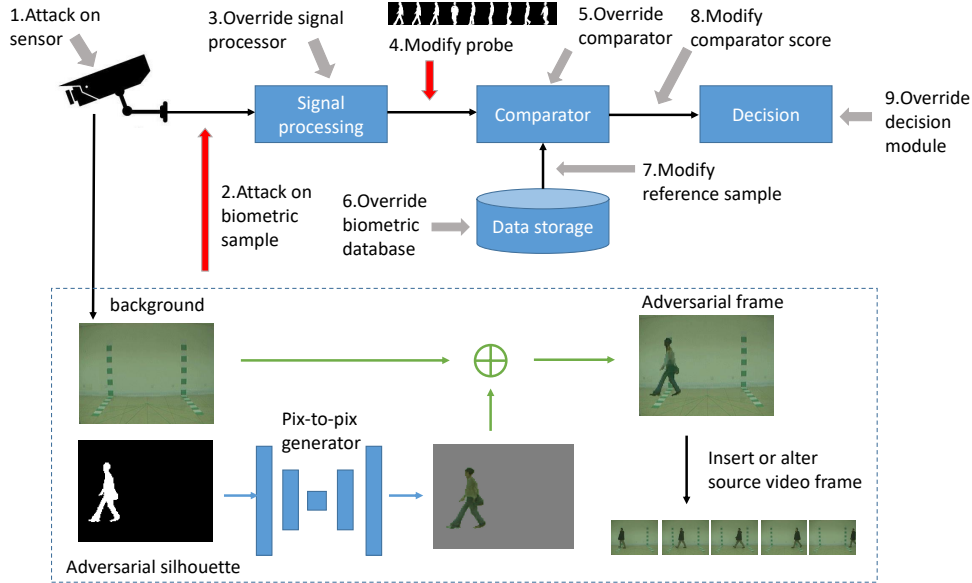


Figure 3. Vulnerability of a biometric recognition system. This figure is inspired by Jia et al. [15]. Our method can be applied in both the 2nd and 4th step. To attack on biometric samples, we train a generator to translate an adversarial silhouette image into a valid video frame.

gorithms such as background difference. Moreover, some sequence-based models, like GaitSet, are flexible and capable of containing non-consecutive silhouettes in input sets. Thus, in these scenarios our temporal sparse adversarial video is not easy to detect; our video can cause a real threat to practical applications.

## 4. Experiments

In this section, we conduct experiments to explore the vulnerability of gait recognition models under our temporal sparse attack. First, we specify the experimental settings in Sec. 4.1. Then, we test the adversarial robustness of the state-of-the-art gait recognition model via the proposed method. The white-box setting is presented in Sec. 4.2 and a cross-dataset validation is presented in Sec. 4.4. We also perform a black-box attack to investigate whether adversarial examples of sequence-based models can transfer to template-based models in Sec. 4.3. Finally, we provide a comparison of the proposed method with existing perturbation-based methods to demonstrate the superiority of our method in Sec. 4.5.

### 4.1. Setup

**Datasets.** We conduct experiments on two datasets, CASIA-A [35] and CASIA-B [35]. CASIA-A consists of 20 subjects, and each subject has 12 sequences under three viewing angles, labeled with 00\_1, 00\_2, 00\_3, 00\_4, 45\_1, 45\_2, 45\_3, 45\_4, 90\_1, 90\_2, 90\_3, and 90\_4. CASIA-B is a widely used gait dataset that contains 124 subjects (labeled 001-124) with 11 different viewing angles and 10 sequences

per subject for each view. The 10 sequences contain three walking conditions: six sequences are in the normal walking state (NM 1-6), two sequences contain walking subject wearing coats (CL 1-2), and two sequences contain subject carrying bags (BG 1-2). We mainly use CASIA-B for evaluation and CASIA-A for cross-dataset validation.

Since GaitSet is trained on the first 74 subjects (labeled 1-74) and tested on the remaining 50 subjects of CASIA-B, we follow this setting to attack the last 50 subjects (labeled 75-124). For each subject, the first four sequences of the NM condition (NM 1-4) are kept in the gallery to test the recognition accuracy. All of the frames in a specific view and walking condition are used as a sequence for the test. For the cross-dataset validation, we use the whole CASIA-A. The first three sequences of each angle are in the probe and the fourth sequence is in the gallery. The setting is summarized in Table 1.

**Models.** The attacked model is GaitSet, the state-of-the-art gait recognition model. GaitSet regards the gait as a set of gait silhouettes and utilizes a deep neural network to directly extract temporal information during training. Moreover, GaitSet is flexible since the input set can contain any number of non-consecutive silhouettes.

For the black-box experiments, we use the template-based model GaitGAN [34]. Different from GaitSet, which takes a gait sequence as a set and extracts its feature with a CNN, GaitGAN uses a GEI template as the gait feature. Moreover, GaitGAN takes a GAN model as a regressor to simultaneously address variations in viewpoint, clothing, and carrying conditions in gait recognition.

**Metrics.** We evaluate the vulnerability of gait recogni-

CASIA-B	training set		ID: 001-074 nm01-nm06, bg01-nm02, cl01-cl02,
	gallery set		ID: 075-124 nm01-nm04
	probe set	probeNM	ID: 075-124 nm05,nm06
		probeBG	ID: 075-124 bg01,bg02
probeCL		ID: 075-124 cl01,cl02	
CASIA-A	gallery set		ID:all 00_4, 45_4, 90_4
	probe set	probe 0°	ID:all 00_1, 00_2, 00_3
		probe 45°	ID:all 45_1, 45_2, 45_3
		probe 90°	ID:all 90_1, 90_2, 90_3

Table 1. The dataset setting.

tion models by assessing their accuracy. The accuracy is averaged on all gallery views, and the identical views are excluded. For example, when testing with CASIA-B, the accuracy of the probe view 90° is averaged on 10 gallery views, excluding gallery view 90°.

**Implementation details.** If not specifically mentioned, we conduct nontargeted attack. For targeted attack, we randomly choose the target ID and select one sequence of targeted ID as  $X_t$  in Eq.(3).

For the mask  $M$ , we let the set  $\Phi$  be  $\Phi = \{1, 2, \dots, K\}$ , which means we simply alter the first  $K$  frames with adversarial ones.  $K$  is computed according to the needed sparsity.

WGAN-GP [9] is an important extension of GAN which improves image quality and stabilizes training. We train the WGAN-GP on CASIA-B for 16000 iterations; the trained generator  $G$  and the discriminator  $D$  are used in our attack. We set the dimension of inputted latent variables as  $V = 128$ .

Our attack is based on MIFGSM [5], and the hyperparameters are set as follows: the iterations are 100,  $\lambda = 1000$  in Eq.(5),  $\mu = 1.0$  in Eq.(6),  $\epsilon = 0.1$  in Eq.(7).

SPADE [23] is a method based on conditional normalization, and it can convert the segmentation map to a photo-realistic image. We use the SPADE in the silhouettes to video translation. We train it on CASIA-B for 670000 iterations.

**Settings for perturbation methods.** For comparison, we report the experimental results under the attack setting as the 4th step in Fig. 3. For perturbation-based methods, we choose FGSM, PGD, and MIFGSM as baselines. The distortion budget is set to the value 1 for these methods, with

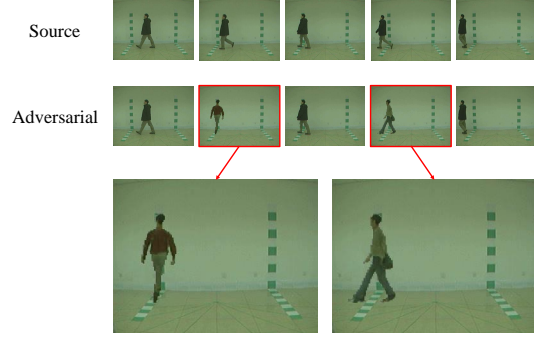


Figure 4. One example of generated videos.

the pixel value within  $[0,1]$ . For iterative methods, PGD and MIFGSM, the iterations are set to 20. The decay factor in MIFGSM is set as 1.0.

## 4.2. White-box experiments

In this subsection, we attack GaitSet under the white-box protocol. This means we have the full knowledge of the target model. For clarity, we report the results of frame-alteration attack and leave the results of frame-insertion attack in supplementary materials as the trends for both methods are similar. For our attack on biometric samples, we list some generated frames in Fig. 4.

**Nontargeted results.** We report the results of our attack under nontargeted setting in Fig.5. We observe that our attacks with different sparsity successfully deceive GaitSet, causing low accuracy in all three walking conditions. Moreover, the attack success rate is positively correlated with sparsity, which means that a stronger attack needs more modified frames in a sequence. However, the accuracy drops dramatically when the sparsity is 1/40.

To further prove the drop accuracy is caused by our novel attack design rather than altering some frames with randomly chosen gait silhouettes, we compare two situations: (1) *Random*. The latent variable  $z$  is randomly sampled from a standard Gaussian distribution. (2) *Adversary*. The latent variable  $z$  is obtained by our adversarial attack. As shown in Fig. 5, *Random* only slightly affects the accuracy of GaitSet, while *Adversary* has more severe damage to the recognition performance. These results demonstrate the effectiveness of our attack. One intriguing phenomenon is that the *Random* or *Adversary* settings have a more obvious effect on the accuracy when the view angle is close to 0° or 180°. Under these conditions, the attack is hardly recognizable. These remain challenging cases for most of the state-of-the-art gait recognition methods.

**Targeted results.** We report the results of targeted attack in Table 2. Compared with nontargeted one, targeted attack is apparently more difficult, because it aims to deceive the gait recognition system with a specific subject ID

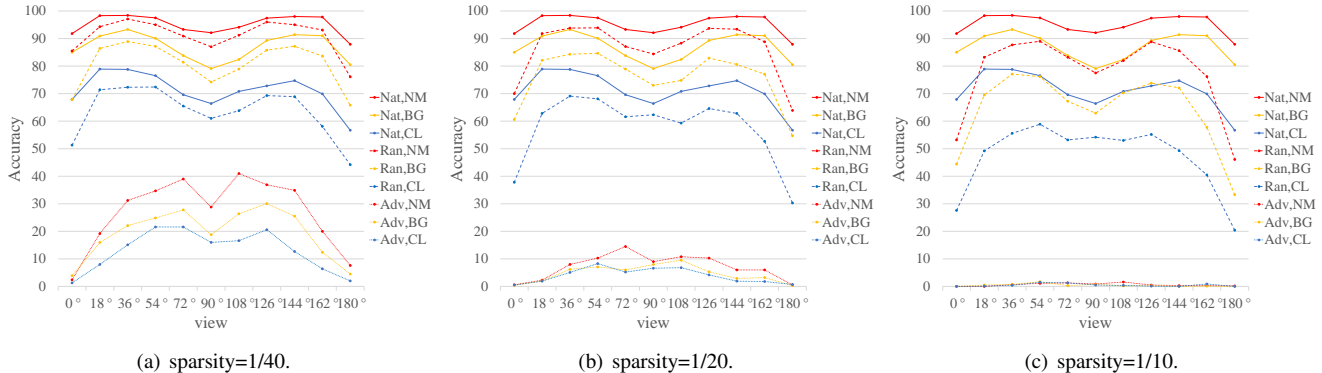


Figure 5. Results of white-box nontargeted attack. Predefined sparsity includes 1/10, 1/20, and 1/40. Three walking conditions are labeled with different colors and three settings (Natural (Nat), Random (Ran), and Adversary (Adv)) are labeled with different line types.

sparsity	walking condition		
	NM	BG	CL
1/40	15.118	18.504	22.927
1/20	37.627	43.201	45.509
1/10	65.636	67.978	69.300

Table 2. Results of white-box targeted attack, shown as attack success rate(%).

rather than any one. Nonetheless, the proposed method can successfully deceive the GaitSet with a high rate at around 65% when the sparsity is 1/10. Therefore, our method can serve as a strong benchmark of adversarial attack on gait recognition.

### 4.3. Black-box experiments

Our attack method is specifically aimed at sequence-based gait recognition models, and the above experimental results demonstrate their vulnerability. In this subsection, we also make a black-box attack on the template-based model, GaitGAN [34]. In this scenario, we cannot access any information of the target model in the attack process. To perform the black-box attack, we attack GaitSet to obtain the adversarial sequence first, and then use GaitGAN for testing.

The sparsity is 1/40 and the adversarial sequences are the same as Adv, NM in Fig. 5(a). We report the results of probeNM, shown in Table 3. The recognition rate of each probe view only drops a little after attacking. We conclude that GEI is more robust than the feature extracted by GaitSet under our temporal adversarial attack. Because GEI is obtained by aligning the silhouettes in the spatial space and averaging them along the temporal dimension, the perturbation of a few frames is not enough to deceive GaitGAN. Although sequence-based gait recognition has made great progress in recognition accuracy, its robustness compared to template-based methods remains limited. This is a key

area for the community to focus on in the future.

### 4.4. Cross-dataset validation

For a more reliable performance assessment, we conduct cross-database testing using CASIA-A. In this scenario, the training set of CASIA-B is used to train the GaitSet and WGAN-GP, while the whole CASIA-A dataset is used for testing. Results are shown in Table 4. The accuracy is averaged on the 3 gallery views, and the identical views are included. The trend is almost the same as the results of testing on CASIA-B. The recognition capability of the attacked model drops rapidly as the attack sparsity increases. When the sparsity is 1/40, the attack success rate reaches 58.2% on average.

### 4.5. Comparison with perturbation-based methods

In Sec. 1, we have qualitatively demonstrated the shortcomings of the perturbation-based approaches. In this subsection, we compare our proposed method with these methods quantitatively. The perturbation-based attacks used as baselines include FGSM [8], PGD [19] and MIFGSM [5]. It is difficult to extend these attacks to video frame generation due to the signal processing in silhouette-based gait recognition. Therefore, in this study we perform attacks on the gait silhouettes. For a fair comparison, we fix the sparsity; the attack success rate and imperceptibility of adversarial examples generated by different methods are compared. The distortion budgets of perturbation-based methods are all relaxed to pixel values, which means adversarial examples are not norm-bounded by a small constant for these methods. Our method is under the protocol of a frame-alteration attack.

The results are shown in Fig. 6, and some crafted adversarial examples are shown in Fig. 7. Our proposed method achieves a superior attack success rate and imperceptibility. In Fig. 6, we observe that while all of the attacks lower the accuracy of GaitSet, our method surpasses the perturbation-

probe view	0	18	36	54	72	90	108	126	144	162	180	average
natural	39.4	56.0	62.3	61.1	59.3	25.8	55.8	63.6	57.3	52.9	40.7	52.2
after attack	35.9	52.8	60.0	57.6	56.1	24.4	52.2	60.4	55.2	49.5	36.2	49.1
drop ↓	3.5	3.2	2.3	3.5	3.2	1.4	3.6	3.2	2.1	3.4	4.5	3.1

Table 3. Results of a Black-box attack on GaitGAN, shown as accuracy(%).

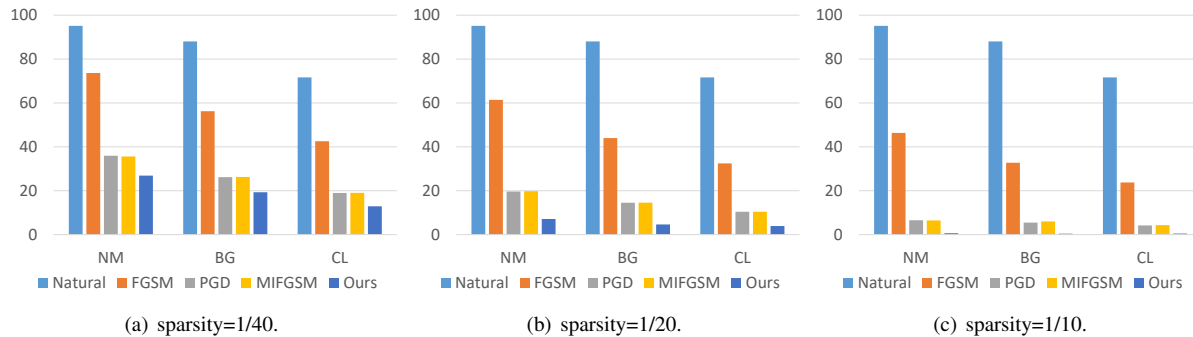


Figure 6. Comparison of our method with perturbation-based methods. ‘Natural’ is the original accuracy of GaitSet and others represent the accuracy under attack.

sparsity	probe view			
	0°	45°	90°	average
0	56.67	70.00	76.67	67.78
1/40	33.33	33.33	18.33	28.33
1/20	18.33	25.00	3.33	15.55
1/10	6.67	8.33	3.33	5.11

Table 4. Results of cross-database validation, shown as accuracy(%).

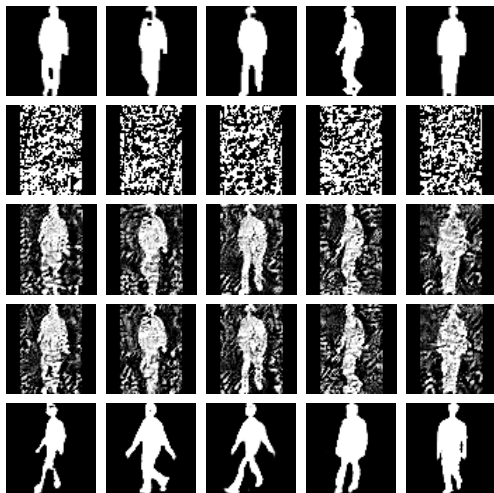


Figure 7. From top to bottom are natural examples and their corresponding adversarial examples generated by FGSM, PGD, MIFGSM, and our method.

based methods by obtaining superior attack success rates in all of the settings. In Fig. 7, we show that the subjects in the

silhouettes retain a human posture in our method. Thus, it maintains better imperceptibility of the spatial domain than perturbation-based methods. Furthermore, it enables the transfer of these silhouettes to video frames; it makes a practical threat to the gait recognition system. However, a limitation is that the generated samples have pose changes when they are compared to their adjacent frames. Therefore, some constraints are needed to enforce the changes between the adjacent frames, which we leave for our future work. Compared with perturbation-based methods, our proposed method provides superior success rates and imperceptibility and can serve as a stronger baseline for sequence-based gait recognition.

## 5. Conclusion

In this paper, we propose a novel temporal sparse adversarial attack on gait recognition. Our method achieves good imperceptibility and a high attack success rate. Experiments on CASIA datasets indicate that the state-of-the-art model, GaitSet, is vulnerable to our adversarial attack. This reveals a key limitation in adversarial robustness research on gait recognition that requires urgent attention. Our method also shows a potential threat in practical applications as it is flexible in either attacking on biometric samples captured by a sensor or directly modifying probes. We mainly focus on the vulnerability of sequence-based models and show template features like GEI may resist our attack. The results highlight the inherent loss of temporal and fine-grained spatial information in gait templates; consequently, they can avoid deliberate attacks on vulnerable temporal features. Therefore, we identify the need for the community to con-

sider the robustness of sequence-based methods, which possess the benefit of high accuracy, in future research.

## References

- [1] Martín Arjovsky, Soumith Chintala, and Léon Bottou. Wasserstein GAN. *Arxiv*, abs/1701.07875, 2017. 3
- [2] Tom B. Brown, Nicholas Carlini, Chiyuan Zhang, Catherine Olsson, Paul Francis Christiano, and Ian J. Goodfellow. Unrestricted adversarial examples. *ArXiv*, abs/1809.08352, 2018. 2, 3
- [3] Hanqing Chao, Yiwei He, Junping Zhang, and Jianfeng Feng. Gaitset: Regarding gait as a set for cross-view gait recognition. In *Proceedings of the AAAI Conference on Artificial Intelligence*, pages 8126–8133, 2019. 2
- [4] Zhikai Chen, Lingxi Xie, Shanmin Pang, Yong He, and Qi Tian. Appending adversarial frames for universal video attack. *ArXiv*, abs/1912.04538, 2019. 2
- [5] Yinpeng Dong, Fangzhou Liao, Tianyu Pang, Hang Su, Jun Zhu, Xiaolin Hu, and Jianguo Li. Boosting adversarial attacks with momentum. In *IEEE Conference on Computer Vision and Pattern Recognition*, pages 9185–9193, 2018. 2, 4, 6, 7
- [6] Davronzhon Gafurov, Einar Sneekkenes, and Patrick Bours. Spoof attacks on gait authentication system. *IEEE Trans. Information Forensics and Security*, pages 491–502, 2007. 1
- [7] Ian J. Goodfellow, Jean Pouget-Abadie, M. Mirza, Bing Xu, David Warde-Farley, Sherjil Ozair, Aaron C. Courville, and Yoshua Bengio. Generative adversarial nets. In *Advances in Neural Information Processing Systems*, pages 2672–2680, 2014. 3
- [8] Ian J. Goodfellow, Jonathon Shlens, and Christian Szegedy. Explaining and harnessing adversarial examples. In *International Conference on Learning Representations*, 2015. 1, 2, 7
- [9] Ishaan Gulrajani, F. Ahmed, Martín Arjovsky, Vincent Dumoulin, and Aaron C. Courville. Improved training of wasserstein gans. In *Advances in Neural Information Processing Systems*, pages 5767–5777, 2017. 3, 6
- [10] Abdenour Hadid, Mohammad Ghahramani, Vili Kellokumpu, Xiaoyi Feng, John D. Bustard, and Mark S. Nixon. Gait biometrics under spoofing attacks: an experimental investigation. *J. Electronic Imaging*, 24(6):063022, 2015. 1
- [11] Abdenour Hadid, Mohammad Ghahramani, Vili Kellokumpu, Matti Pietikäinen, John D. Bustard, and Mark S. Nixon. Can gait biometrics be spoofed? In *International Conference on Pattern Recognition*, pages 3280–3283, 2012. 1
- [12] Ju Han and Bir Bhanu. Individual recognition using gait energy image. *IEEE Transactions on Pattern Analysis and Machine Intelligence*, 28:316–322, 2006. 2
- [13] Yiwei He, Junping Zhang, Hongming Shan, and Liang Wang. Multi-task gans for view-specific feature learning in gait recognition. *IEEE Transactions on Information Forensics and Security*, 14:102–113, 2019. 1, 2
- [14] Phillip Isola, Jun-Yan Zhu, Tinghui Zhou, and Alexei A. Efros. Image-to-image translation with conditional adversarial networks. In *IEEE Conference on Computer Vision and Pattern Recognition*, pages 5967–5976, 2017. 3
- [15] Meijuan Jia, Hongyu Yang, Di Huang, and Yunhong Wang. Attacking gait recognition systems via silhouette guided gans. In *Proceedings of the 27th ACM International Conference on Multimedia*, pages 638–646, 2019. 1, 5
- [16] Tero Karras, Samuli Laine, and Timo Aila. A style-based generator architecture for generative adversarial networks. In *IEEE Conference on Computer Vision and Pattern Recognition*, pages 4401–4410, 2019. 2
- [17] Alexey Kurakin, Ian J. Goodfellow, and Samy Bengio. Adversarial machine learning at scale. *ArXiv*, abs/1611.01236, 2016. 2
- [18] Rijun Liao, Chunshui Cao, Edel B Garcia, Shiqi Yu, and Yongzhen Huang. Pose-based temporal-spatial network (ptsn) for gait recognition with carrying and clothing variations. In *Chinese Conference on Biometric Recognition*, pages 474–483, 2017. 1, 2
- [19] Aleksander Madry, Aleksandar Makelov, Ludwig Schmidt, Dimitris Tsipras, and Adrian Vladu. Towards deep learning models resistant to adversarial attacks. *ArXiv*, abs/1706.06083, 2017. 1, 2, 7
- [20] Sachit Menon, Alexandru Damian, Shijia Hu, Nikhil Ravi, and Cynthia Rudin. PULSE: self-supervised photo upsampling via latent space exploration of generative models. In *IEEE Conference on Computer Vision and Pattern Recognition*, pages 2434–2442, 2020. 3
- [21] Seyed-Mohsen Moosavi-Dezfooli, Alhussein Fawzi, and Pascal Frossard. Deepfool: A simple and accurate method to fool deep neural networks. In *IEEE Conference on Computer Vision and Pattern Recognition*, pages 2574–2582, 2016. 2
- [22] Nicolas Papernot, Patrick D. McDaniel, Somesh Jha, Matt Fredrikson, Z. Berkay Celik, and Ananthram Swami. The limitations of deep learning in adversarial settings. In *IEEE European Symposium on Security and Privacy*, pages 372–387, 2016. 2
- [23] Taesung Park, Ming-Yu Liu, Ting-Chun Wang, and Jun-Yan Zhu. Semantic image synthesis with spatially-adaptive normalization. In *IEEE Conference on Computer Vision and Pattern Recognition*, pages 2337–2346, 2019. 3, 4, 6
- [24] Omid Poursaeed, Tianxing Jiang, Harry Yang, Serge J. Belongie, and Ser-Nam Lim. Fine-grained synthesis of unrestricted adversarial examples. *ArXiv*, abs/1911.09058, 2019. 2, 3
- [25] Mahmood Sharif, Sruti Bhagavatula, Lujio Bauer, and Michael K Reiter. Accessorize to a crime: Real and stealthy attacks on state-of-the-art face recognition. In *Proceedings of the 2016 ACM SIGSAC Conference on Computer and Communications Security*, pages 1528–1540, 2016. 1
- [26] Kohei Shiraga, Yasushi Makihara, Daigo Muramatsu, Tomio Echigo, and Yasushi Yagi. Geinet: View-invariant gait recognition using a convolutional neural network. In *International Conference on Biometrics*, pages 1–8, 2016. 2
- [27] Yang Song, Rui Shu, Nate Kushman, and Stefano Ermon. Constructing unrestricted adversarial examples with generative models. In *Advances in Neural Information Processing Systems*, pages 8312–8323, 2018. 2

- [28] Christian Szegedy, Wojciech Zaremba, Ilya Sutskever, Joan Bruna, Dumitru Erhan, Ian J. Goodfellow, and Rob Fergus. Intriguing properties of neural networks. In *International Conference on Learning Representations*, 2014. 1
- [29] Noriko Takemura, Yasushi Makihara, Daigo Muramatsu, Tomio Echigo, and Yasushi Yagi. On input/output architectures for convolutional neural network-based cross-view gait recognition. *IEEE Transactions on Circuits and Systems for Video Technology*, 29:2708–2719, 2019. 1, 2
- [30] Xingxing Wei, Jun Zhu, and Hang Su. Sparse adversarial perturbations for videos. In *Proceedings of the AAAI Conference on Artificial Intelligence*, pages 8973–8980, 2018. 2, 3
- [31] Thomas Wolf, Mohammadreza Babaei, and Gerhard Rigoll. Multi-view gait recognition using 3d convolutional neural networks. In *IEEE International Conference on Image Processing*, pages 4165–4169, 2016. 1, 2
- [32] Zifeng Wu, Yongzhen Huang, Liang Wang, Xiaogang Wang, and Tieniu Tan. A comprehensive study on cross-view gait based human identification with deep cnns. *IEEE Transactions on Pattern Analysis and Machine Intelligence*, 39:209–226, 2016. 1, 2
- [33] Cihang Xie, Jianyu Wang, Zhishuai Zhang, Yuyin Zhou, Lingxi Xie, and Alan L. Yuille. Adversarial examples for semantic segmentation and object detection. In *IEEE International Conference on Computer Vision*, pages 1378–1387, 2017. 1
- [34] Shiqi Yu, Haifeng Chen, Edel B. García Reyes, and Norman Poh. Gaitgan: Invariant gait feature extraction using generative adversarial networks. In *IEEE Conference on Computer Vision and Pattern Recognition Workshops*, pages 532–539, 2017. 2, 5, 7
- [35] Shiqi Yu, Daoliang Tan, and Tieniu Tan. A framework for evaluating the effect of view angle, clothing and carrying condition on gait recognition. In *International Conference on Pattern Recognition*, pages 441–444, 2006. 2, 5

## A. Experimental details

**Datasets.** CASIA-A is an outdoor gait database including 20 persons. Each person has 12 image sequences, 4 sequences for each of the three directions, i.e. parallel, 45 degrees and 90 degrees to the image plane. The length of each sequence is not identical for the variation of the walker’s speed, but it must range from 37 to 127.

CASIA-B is a large multiview gait database. There are 124 subjects, and the gait data was captured from 11 views. Three variations, namely view angle, clothing and carrying condition changes, are separately considered.

The above datasets can be downloaded from <http://www.cbsr.ia.ac.cn/english/Gait%20Databases.asp>. The silhouettes are released publicly but videos are not. To download the video files, you should sign an agreement and follow its steps.

**WGAN-GP.** WGAN-GP is an important extension of GAN which improves image quality and stabilizes training.

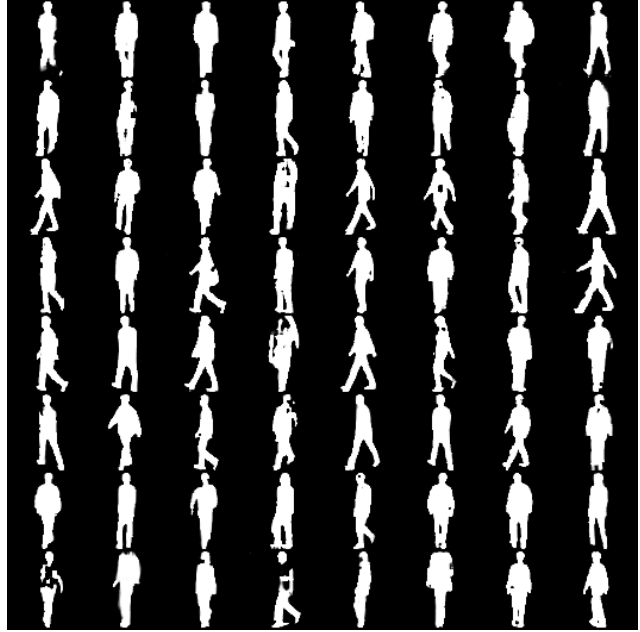


Figure 8. Generated examples of WGAN-GP.

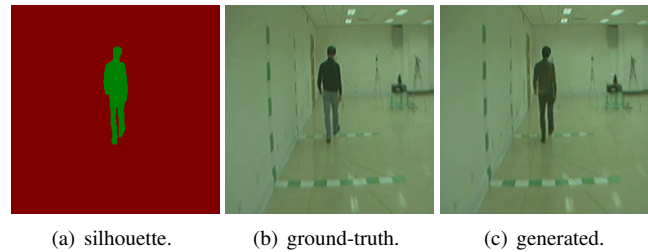


Figure 9. Examples of SPADE.

We use a PyTorch implementation of <https://github.com/jalola/improved-wgan-pytorch>. We train it on CASIA-B for 16000 iterations and show some generated examples in Fig.8.

**SPADE.** SPADE is a method based on conditional normalization, and it can convert the segmentation map to a photo-realistic image. We use the implementation provided by the original paper and the code is in <https://github.com/NVlabs/SPADE>. We train it on CASIA-B for 670000 iterations and show some examples in Fig.9.

## B. Detail results

We report the results of frame-insertion white-box attack here, for nontargeted and targeted settings, in Fig.10 and Table 5, respectively. The trend is similar to frame-alteration attack. We list the detail results of targeted frame-alteration attack in Table 6.

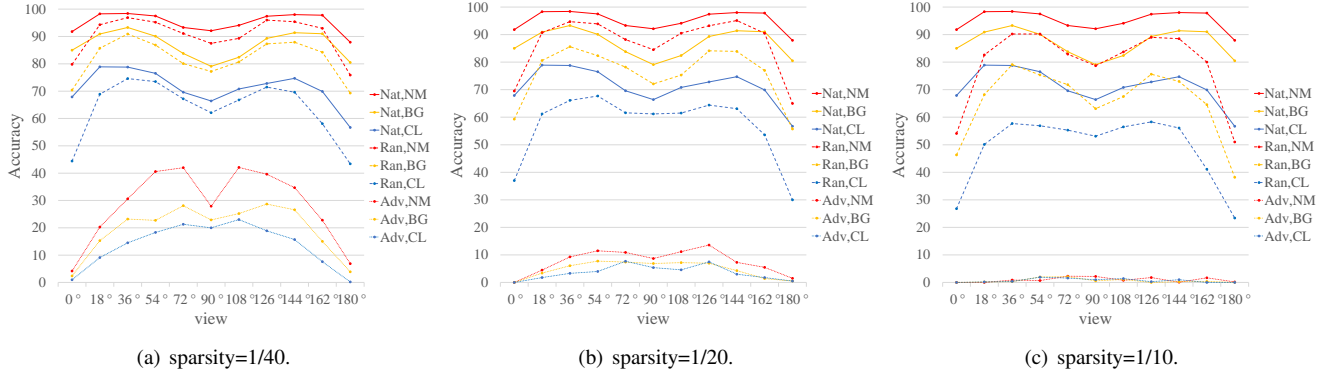


Figure 10. Results of the **frame-insertion** nontargeted attack. Predefined sparsity includes 1/10, 1/20, and 1/40. Three walking conditions are labeled with different colors and three settings (Natural (Nat), Random (Ran), and Adversary (Adv)) are labeled with different line types.

sparsity		view											average
		0	18	36	54	72	90	108	126	144	162	180	
1/40	NM	32.00	16.50	11.90	9.80	8.90	11.50	6.60	8.70	9.90	18.00	32.20	15.091
	BG	33.20	19.50	14.80	14.04	12.50	15.90	8.90	11.60	14.60	20.81	36.90	18.431
	CL	42.20	23.20	16.70	14.80	12.50	16.80	16.70	16.30	22.90	28.00	40.40	22.773
1/20	NM	58.70	43.10	34.40	27.90	24.80	26.80	24.80	25.30	31.30	39.70	58.80	35.964
	BG	65.10	45.50	38.80	31.82	28.70	32.70	30.70	33.70	41.00	46.06	59.70	41.252
	CL	62.80	50.30	37.40	34.70	31.60	37.70	32.50	38.70	45.60	51.50	63.00	44.164
1/10	NM	77.00	65.80	60.20	58.40	53.40	57.50	56.40	58.60	62.20	67.70	76.60	63.073
	BG	80.10	68.50	63.40	60.00	58.10	59.90	57.70	62.80	65.70	69.70	77.00	65.718
	CL	81.20	72.00	64.30	62.40	60.60	63.50	61.30	61.60	67.60	70.90	80.50	67.809

Table 5. Success rate (%) of the **frame-insertion** targeted attack.

sparsity		view											average
		0	18	36	54	72	90	108	126	144	162	180	
1/40	NM	34.60	18.90	13.20	8.60	7.70	9.40	7.90	10.10	8.30	16.80	30.80	15.118
	BG	31.70	20.70	14.60	11.41	11.70	14.40	12.40	12.10	16.10	22.93	35.50	18.504
	CL	42.30	23.40	17.20	17.50	13.10	17.90	15.70	14.90	23.20	26.00	41.00	22.927
1/20	NM	61.60	43.40	33.30	30.50	25.40	29.00	22.20	27.90	37.00	40.10	63.50	37.627
	BG	63.30	47.00	39.50	34.64	33.40	37.30	33.00	36.10	41.10	47.07	62.80	43.201
	CL	65.60	49.20	39.50	37.80	35.70	36.20	36.30	38.60	47.20	50.70	63.80	45.509
1/10	NM	78.60	67.40	59.40	61.40	60.00	61.10	58.90	60.90	65.10	68.60	80.60	65.636
	BG	82.30	69.80	65.40	64.55	61.20	62.90	60.50	63.50	66.50	70.91	80.20	67.978
	CL	78.90	70.50	63.80	66.20	62.40	65.00	65.50	65.70	69.90	73.10	81.30	69.300

Table 6. Success rate (%) of the **frame-alteration** targeted attack.